# *EWS-FLI1 is incorporated into a protein granule in cells*

*Nasiha S. Ahmed[1], Lucas M. Harrell[2], Jacob Schwartz[2*]*

[1] Department of Molecular and Cellular Biology, The University of Arizona, Tucson, AZ 85719

[2] Department of Chemistry and Biochemistry, The University of Arizona, Tucson, AZ 85719

* Corresponding author: jcschwartz@email.arizona.edu

Keywords: Ewing sarcoma, FET proteins, fusion proteins, phase-separation, granules, intrinsically disordered domains

**ABSTRACT**

Ewing sarcoma is driven by fusion proteins containing a low complexity (LC) domain that is intrinsically disordered and a powerful transcription regulator. The most common fusion protein found in Ewing sarcoma, EWS-FLI1, takes its LC domain from the RNA-binding protein EWSR1 (Ewing Sarcoma RNA-binding protein 1) and a DNA-binding domain from the transcription factor FLI1 (Friend Leukemia Virus Integration 1). The LC domain in EWS-FLI1 can bind RNA polymerase II (RNA Pol II) and can self-assemble through a process known as phase separation. The ability of EWSR1 and related RNA-binding proteins to assemble into ribonucleoprotein granules in cells has been vigorously studied and while many questions remain, the role of phase separation in EWS-FLI1 activity is less understood. We investigated the overlapping functions of EWSR1 and EWS-FLI1 in controlling gene expression and tumorigenic cell growth in Ewing sarcoma, which suggested these proteins function closely together. We then studied the nature of interactions between EWS-FLI1, EWSR1, and RNA Pol II. We observed EWSR1 and RNA Pol II to be present in protein granules in cells. We then identified protein granules in cells associated with the fusion protein, EWS-FLI1. The tyrosine residues in the LC domain are required for both the abilities of EWS-FLI1 to bind its partners, EWSR1 and RNA Pol II, and to incorporate into protein granules. These data suggest that interactions between EWS-FLI1, RNA Pol II, and EWSR1 in Ewing sarcoma can occur in the context of a molecular scaffold found within protein granules in the cell.

## INTRODUCTION

RNA-binding proteins are key players in every step of mRNA biogenesis[1]. The FET proteins are a family of highly homologous and ubiquitously expressed RNA-binding proteins comprised of FUS, EWSR1, and TAF15. These proteins are predominantly nuclear and bind thousands of RNA with degenerate specificity[1,2]. While significantly more published work has focused on FUS activities in cells, recent studies have begun to shed light on the properties and functions of EWSR1. A number of cellular functions of the FET proteins overlap, such as the regulation of expression from thousands of genes[3–6]. FUS and EWSR1 each bind the C-terminal domain (CTD) of RNA Pol II and modulation phosphorylation of the domain[7–9]. EWSR1 has also been shown to bind nascent RNA transcripts, a number of RNA processing factors, and transcription factors[10,11]. This extensive network of interactions maintained by FET proteins provide them several avenues that broadly affect gene expression[4,12,13].

The FET protein genes are frequently involved in genomic translocation events in sarcomas[14,15]. The second most common pediatric bone cancer is Ewing sarcoma. These tumors result from a translocation event that fuses the N-terminal low complexity (LC) domain of a FET protein and the DNA-binding domain (DBD) of an ETS transcription factor. For 85% of Ewing sarcomas, the LC domain of EWSR1 and the DBD from the FLI1 combine to form the oncogenic protein EWS-FLI1[16,17]. Ewing sarcoma is generally considered to arise from mesenchymal stem cells[18,19]. Expression of EWS-FLI1 is sufficient for transformation in Ewing sarcoma[20,21]. The FLI1 DBD in EWS-FLI1 recognizes a short DNA sequence GGAA and functions most efficiently for enhancer regions containing 10 or more repeats of the motif[22,23]. Like the wild-type FET proteins, EWS-FLI1 binds RNA Pol II, as well as a number of transcription factors and enhancer or repressor complexes[24–27]. Nevertheless, the mechanism for EWS-FLI1 to broadly modulate transcription remains incomplete.

A striking property of FET proteins is their ability to assemble into higher-order ribonucleoprotein (RNP) assemblies in a process known as phase separation[8,28]. RNA seeds this assembly process and it is the oligomerized protein that binds RNA Pol II[8,29]. The LC domains of FET proteins contain a number of repeated [S/G]Y[S/G] motifs. The tyrosine residues contained in this motif are critical for the domain to

undergo phase separation[8,26,28]. In cells, phase separation gives rise to several RNP granules. Examples include stress granules and p-bodies in the cytoplasm and nucleoli in the nucleus. Several recent studies have provided evidence for phase separation to modulate transcription[30]. FET proteins would naturally be predicted to be involved in this form of transcription control[31–33].

The LC domain contained in EWS-FLI1 has transferred the ability to phase separate to the fusion protein[26,34]. EWS-FLI1 binds and recruits EWSR1 to enhancer regions and assemblies formed by the fusion protein interact with RNA Pol II[26,35,36]. Interestingly, the homotypic self-interactions of the LC domain are required to stabilize EWS-FLI1 binding at GGAA microsatellites in cells. Phase separation by EWS-FLI1 along chromosomal DNA is also required for the fusion protein to control transcription and initiate transformation. Our lab has shown FUS and RNA Pol II interact with each other in a nuclear granule[5,37]. The role that phase separation plays in the functions of FET-fusion proteins suggests that they may also incorporate into protein granules in cells.

We investigated the ability of EWS-FLI1 to associate with protein granules in cells. We first extended the body of evidence to support that EWSR1 cooperates with EWS-FLI1 to modify gene expression and cell transformation. Subsequently, we applied crosslinking-based methods to explore whether EWSR1 and EWS-FLI1 occupy large protein particles in cells. The importance of this study is to augment understanding of the role of EWS-FLI1 phase separation in transcription and transformation by charactering the physical properties of the structures formed in cells.

## METHODS

### Cell Culture

Cell lines were obtained from ATCC. A673 and SK-N-MC cells were grown in DMEM (Corning) supplemented with 10% FBS. HEK293T/17 cells were grown in DMEM supplemented with 5% FBS. All cell lines were cultured at 37°C and 5% $CO_2$.

**Plasmid and siRNA Transfections**

The siRNAs used were siSCR 5'–GAUGCAGACAUUCAGGAUGUU–3′; siEF 5'–GCUUCUAGUAGUAGCUGCCUU–3'; siEWSR1 5'–CUACUAGAUGCAGAGACCCUU–3'; siE-EF 5'–GACCGCCUAUGCAACUUCUUU–3'. All siRNAs were annealed to its complement strand. The plasmids used, pLV-V5-EWS-FLI1 and pLV-V5-EWS(YS37)-FLI1, were a gift from the M. Rivera Lab. For siRNA transfections, A673 cells were reverse transfected at 5.0 x $10^5$ cells in 6-well dishes using Lipofectamine™ RNAiMAX (ThermoFisher, cat#13778075) according to manufacturer's instructions. HEK293T/17 and SK-N-MC cells were plated at 4.0 x $10^5$ in 6-well dishes 24 hours prior to transfection using the TransIT-X2 reagent (Mirus Bio cat#MIR6000) or RNAiMAX. All siRNA transfections were at a final concentration of 50 nM and cells were harvested 48–72 hours post-transfection for analysis by western blot. For plasmid transfections, HEK293T/17 cells were transfected at 80% confluency. Cells were transfected using TransIT-X2 reagent following manufacturer's instructions. Cells were harvested 48–96 hours post-transfection.

**Western Blot Analysis**

Protein lysates concentrations were quantified using BCA Protein Assay (Pierce, Cat. #23227). Protein samples of 5–10 µg were loaded onto 7.5% SDS-PAGE gels. Blots were transferred at 500 mA, blocked in 5% nonfat dried milk in TBS-T, and incubated overnight with primary antibody at 4°C. Blots were washed in TBS-T, incubated in secondary antibody for 1 hour at room temperature, washed again in TBS-T, and imaged after the addition of SuperSignal™ West Pico PLUS Chemiluminescent substrate (ThermoFisher, Cat. #34578). Antibodies used in western blots were anti-EWSR1 (Santa Cruz Biotechnology, Cat. #398318), anti-FLI1 (Abcam, Cat. #15289), anti-RNA Pol II (clone CTD4H8, EMD Millipore, Cat. #05-623), anti-RNA Pol II CTD phospho S5 (Abcam, Cat. #5131), anti-V5 (Abcam, Cat. #27671); secondary antibodies used were donkey anti-mouse IgG HRP (Jackson ImmunoResearch, Cat. #715-035-15) and donkey anti-rabbit IgG HRP (Jackson ImmunoResearch, Cat. #711-035-152).

**RNA Sequencing**

A673 cells were transfected with 50 nM siRNA as described above. Cells were collected 72 hours post-transfection and total RNA was extracted using TRIzol reagent (ThermoFisher, Cat. #15596026). 1 μg of total RNA was prepared for sequencing using NEBNext Poly(A) mRNA Magnetic Isolation Module (NEB, #E7490) to generate sequencing libraries according to manufacturer's instructions.

**Soft Agar Colony Formation Assay**

A673, SK-N-MC, and HEK293T/17 cells transfected with 50 nM siRNA were harvested 24 hours post-transfection. HEK293T/17 cells transfected with 50 nM siRNA and 2 μg of plasmid DNA were harvested 24 hours post-transfection. A673 and SK-N-MC cells were seeded at density of 1.0 x $10^5$ cells. Cells were resuspended in 0.35% agarose in growth media and plated onto a bed of solidified 0.6% agarose in growth media. HEK293T/17 cells were seeded at a density of 20k to 30k cells. Cells were resuspended in 0.4% agarose in growth media onto a bed of solidified 0.6% agarose in growth media. A673 and SK-N-MC cells were grown at 37°C and 5% $CO_2$ for 3–4 weeks, imaged, and then colonies were counted using ImageJ software. HEK293T/17 cells were grown at 37°C and 5% $CO_2$ for 1–2 weeks, imaged, and then colonies were counted. Colonies with stained with 0.05% methylene blue.

**Cell Growth Assay**

A673 cells were reverse transfected at a density of 4.0 x $10^5$ cells in 6-well dishes. Cells were collected by trypsinization and counted on a hemocytometer at 24, 48, 72, and 96-hour time points post-transfection.

**Co-Immunoprecipitation Assay**

Co-immunoprecipitation assays (co-IP) were performed with cells. Cells were harvested from 6-well plates and lysed in co-IP lysis/wash buffer (25 mM Tris-HCl pH 7.4, 200 mM NaCl, 1 mM EDTA, 0.5% NP40,

5% glycerol). Protein A/G agarose beads (EMD Millipore, Cat. #IP05) were incubated with primary antibody for 2 hours at 4°C before addition to cell lysate. Lysate was incubated with beads-antibody complex overnight with rotation at 4°C. Beads were washed five times in co-IP lysis/wash buffer, resuspended in Novex NuPage™ Sample Loading Buffer (Fisher Scientific, Cat. #np0008) with 5 mM DTT, and boiled for 5 minutes at 95°C. Beads were then spun at 8000 rpm to elute protein complexes. co-IP assays were then assessed by western blot.

For crosslinked co-IP assays, cells were harvested from confluent 150 mm dishes. Cells were crosslinked in 1% formaldehyde for 15 minutes and then quenched in 125 mM glycine. Cells were washed in phosphate buffered saline (PBS) and lysed in Buffer B (1% SDS, 10 mM EDTA, 50 mM Tris-HCl pH 8.0) supplemented with protease inhibitors. Lysate was sonicated using the Bioruptor Pico (Diagenode) for 30 minutes and then spun at maximum speed for 30 minutes at 4°C. Crosslinked lysate was diluted 10-fold in IP lysis buffer (0.01% SDS, 1.1% Triton-X, 1.2 mM EDTA, 16.7 mM Tris-HCl pH 8.0, 167 mM NaCl) treated with protease inhibitors (Sigma-Aldrich, Cat. #P8340) and benzonase (Millepore-Sigma, Cat. #70746). Lysate was then incubated with rotation overnight with primary antibody at 4°C. Antibody-bound complexes were immunoprecipitated with Novex DYNAL Dynabeads Protein G (Invitrogen, Cat. #10-003-D) or Protein A/G agarose beads (EMD Millipore, Cat. #IP05) for 2 hours at room temperature. Beads were washed five times using IP lysis buffer and eluted in 3.6 M $MgCl_2$ and 20 mM MES (pH 6.5) for 30 minutes with agitation. IP samples were then assayed for proteins by ELISA.

**Size Exclusion Chromatography**

Protocol for size-exclusion chromatography for crosslinked lysates were prepared as described in Thompson et al[37]. For crosslinked lysates, cells were harvested from confluent 150 mm dishes. Cells were crosslinked in 1% formaldehyde for 15 minutes and then quenched in 125 mM glycine. Cells were harvested by scraping, washed in PBS, and resuspended in 5–10 volumes of Buffer C (400 mM NaCl, 20 mM HEPES pH 7.9, 5% glycerol, 0.75 mM $MgCl_2$, and 6 M urea). Lysates were sonicated for 30 minutes at 4°C, followed by centrifugation at maximum speed at 4°C and then filtered through a Costar Spin-X 0.45 μm

filter (Corning, Cat. #8163). 1–2 mg of lysate was injected onto the column. Size Exclusion chromatography was performed using a Sepharose CL-2B 10/300 column (Sigma-Aldrich, Cat. #CL2B300, 100 mL) injected with lysates from HEK293T/17 or A673 cells. Columns were run in Buffer B (100 mM NaCl, 20 mM HEPES pH 7.9, 0.2 mM EDTA, 5% glycerol, 6 M urea, and 0.5 mM DTT).

**ELISA**

ELISAs were performed in 96-well Greiner LUMITRAC-600 white plates (VWR, Cat. # 82050-724). ELISAs were performed as indirect ELISAs, in which protein samples from SEC or crosslinked immunoprecipitation assays were incubated in plates overnight at 4°C. Afterward, plates were washed three times in Tris buffered saline with 0.1% tween (TBST), blocked for 2 hours at room temperature in 5% nonfat dried milk in TBST, washed four times in TBST and then incubated with primary antibody overnight at 4°C. After incubation with primary antibody, plates were washed four times in TBST and incubated with secondary antibody, goat anti-mouse IgG HRP (ThermoFisher cat#31432) or goat anti-rabbit IgG HRP (ThermoFisher, Cat. #31462) for 1 hour at room temperature. Finally, plates were washed 4 times with TBST and proteins were detected by addition of SuperSignal™ ELISA Femto substrate (ThermoFisher cat# PI37074). Luminescence was read using a BMG POLARstar Omega plate reader or Biotek Neo2 microplate reader.

**Transmission Electron Microscopy**

Carbon Film 300 Mesh Copper grids (Electron Microscopy Sciences, Cat. #CF300-CU) were charged at 15 mA for 30 seconds. Crosslinked immunoprecipitation samples were spotted onto charged grids and stained with 0.75% uranyl formate. For proteinase K treated samples, the samples were treated with 5 μg of proteinase K and incubated for 30 minutes at 37°C before being spotted onto grids and stained with 0.75% uranyl formate. Images were collected from a FEI Tecnai Spirit 120S or FEI Tecnai F20 transmission electron microscope.

## RESULTS

### Transcript levels in Ewing sarcoma are affected by both EWSR1 and EWS-FLI1.

EWSR1 and EWS-FLI1 share the same low-complexity (LC) domain, which undergoes oligomerization for the proteins to regulate transcription[8,26,28]. Previous studies have demonstrated that homotypic self-interactions by the EWS-FLI1 LC domain are required to affect transcription and transformation[8,34,38]. Additionally, EWS-FLI1 recruits EWSR1 to GGAA-rich sites along chromosomal DNA[9,26]. The interaction of the fusion and wildtype LC domain proteins may contribute to their activity in Ewing sarcoma.

We used RNA-seq to determine how many genes were regulated by both EWSR1 and EWS-FLI1. We quantified abundances for poly-adenylated RNA transcripts in a Ewing sarcoma cell line, A673, which expresses *EWS-FLI1* and *EWSR1*. EWS-FLI1 was targeted by a small interfering RNA (siRNA) targeting the 3' region unique to EWS-FLI1 mRNA (siEF), which resulted in 60% EWS-FLI1 protein reduction compared by western blot to a control (siSCR) (**Figure 1A**). EWSR1 was targeted with an siRNA (siEWSR1) targeting its mRNA in the 3' region not shared with EWS-FLI1. Knockdown with siEWSR1 reduced EWSR1 protein by 80% but did not affect EWS-FLI1 protein levels. A third siRNA (siE-EF) depleted both EWSR1 and EWS-FLI1 by targeting the 5' region found in both EWSR1 and EWS-FLI1 mRNAs and reduced levels of each protein by 80% **(Figure 1A).** We did not observe non-specific changes to EWSR1 or EWS-FLI1 protein levels by siEF or siEWSR1, respectively (**Supplemental Figure S1A**).

We assessed by RNA-seq analysis changes in transcript abundance for the top 6932 transcripts expressed in all four treatments. A large fraction of gene transcripts (n = 2026) were increased or decreased in abundance by >1.8-fold following EWS-FLI1 knockdown from siEF. Of those transcripts affected by siEF, 43% were increased in abundance (n = 875) and the remaining decreased (n = 1151). Fewer transcripts changed in abundance following EWSR1 knockdown by siEWSR1 (n = 1073). Of those, a similar 43% saw increased abundance (n = 459) and the remainder were decreased (n = 614). An overlap of transcripts were found to respond similarly to the knockdown of either EWS-FLI1 or EWSR1 knockdown (n = 485,

**Supplemental Figure S1B**). Of those, 58% increased (n = 279) and 33% decreased in their abundance after either knockdown (n = 206) (**Figure 1B**, shown in green). We noted only 54 transcripts were altered in opposing directions for EWS-FLI1 knockdown relative to EWSR1 knockdown (**Figure 1B**, shown in gold).

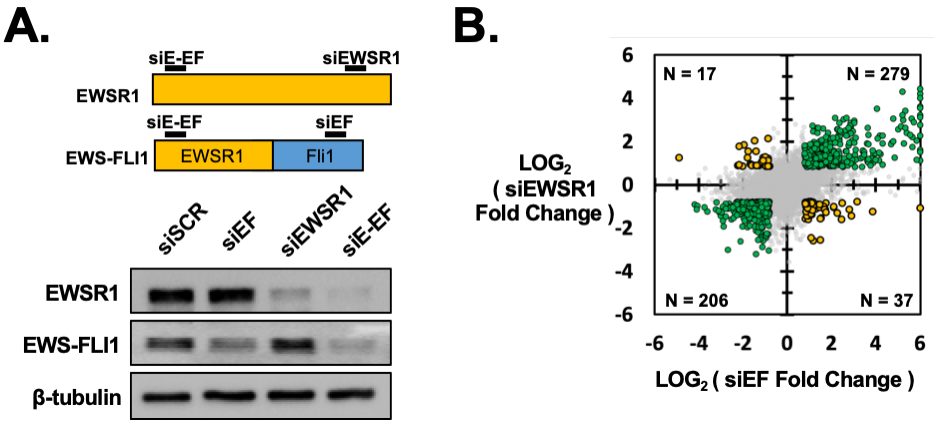


**Figure 1. A large number of transcripts had similar responses after a loss of EWS-FLI1 or EWSR1 in Ewing sarcoma. A.** Schematic of siRNA targets and western blot of confirming knockdown using siRNAs targeted against EWS-FLI1 (siEF), EWSR1 (siEWSR1) or both EWSR1 and EWS-FLI1 (siE-EF) in A673 cells. **B.** A comparison of fold changes revealed 458 transcripts (green) increased or decreased >1.8-fold in the same direction after either EWSR1 or EWS-FLI1 knockdown, and 54 transcripts (yellow) were changed in opposing directions. The number of transcripts changed by more than 1.8-fold are indicated in each quartile.

We compared changes in RNA transcript levels for the loss of the individual proteins to those for the simultaneous loss of EWS-FLI1 and EWSR1. For genes whose transcript abundance responded to the loss of either protein, most (86%, or n = 418) were also changed by a simultaneous knockdown of both. Nearly all genes had the same positive or negative direction for their changes, except for 33 genes whose direction opposed that of the individual knockdowns (**Supplemental Figure S1C**). Taken together, nearly a quarter of gene transcripts controlled by EWS-FLI1 were demonstrated to be under the control of EWSR1. Conversely, nearly half of the gene transcripts responding to the loss of EWSR1 were found to be under

the control of EWS-FLI1. This finding agreed with the hypothesis that EWSR1 and EWS-FLI1 may affect expression for many of the same gene targets.

**EWSR1 is required for anchorage-independent growth in Ewing sarcoma.**

The loss of EWS-FLI1 is known to block anchorage-independent cell growth for Ewing sarcoma cell lines, as seen by the soft agar colony formation assay[39,40]. We tested whether this tumorigenic capacity was also influenced by the EWSR1 protein. If EWS-FLI1 and EWSR1 interactions were functional and significant for Ewing sarcoma biology, a loss of either protein could be expected to result in a similar effect on this important marker of cell transformation.

We quantified growth by cell count for A673 cells after EWSR1 or EWS-FLI1 knockdown. These measurements indicated no change in growth up to 96 hours after transfection, compared to siSCR control (**Supplemental Figure S2A**). Twenty-four hours after siRNA transfection, cells were seeded on soft agar, grown 3 to 4 weeks, and the number of colonies formed were then counted. As expected, the loss of EWS-FLI1 in A673 cells resulted in 60% fewer colonies on the soft agar, compared to siSCR transfection ($n = 3$, $p = 0.04$, Student's t-test, **Figure 2A** and **2B**). Cells with EWSR1 knocked down by siEWSR1 also produced 90% fewer colonies, revealing an EWSR1 dependency for growth on a soft agar substrate ($n = 3$, $p = 0.004$, Student's t-test). We applied the soft agar assay to a second Ewing sarcoma cell line, SK-N-MC, which also expresses EWS-FLI1. Using western blot, knockdown by siEF and siEWSR1 was comparable between SK-N-MC and A673 cells (**Supplemental Figure S2B**). Knockdown produced 80% fewer colonies on soft agar in the SK-N-MC cell line for EWS-FLI1 and 90% fewer colonies for EWSR1 knockdown (**Supplemental Figure S2C and S2D**).

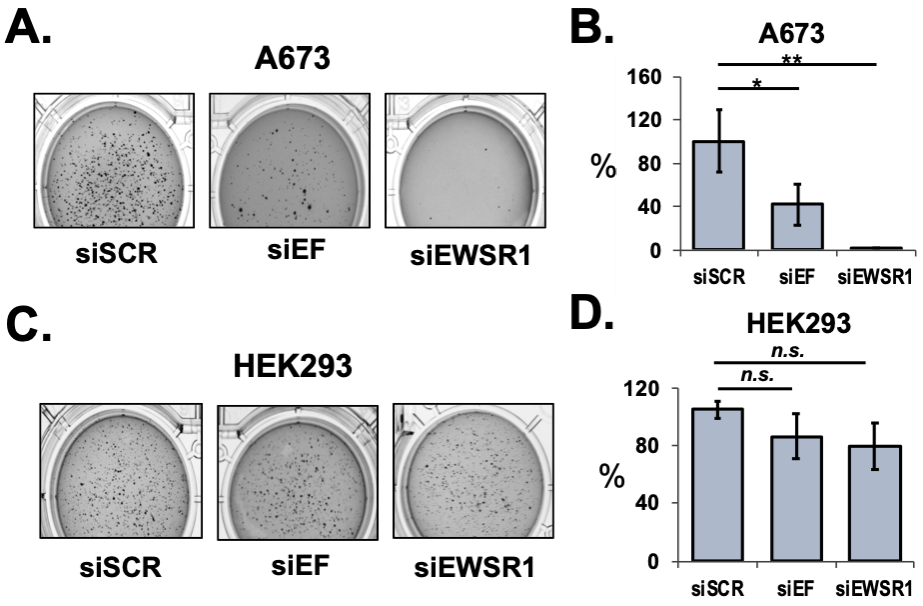


**Figure 2. Loss of EWSR1 inhibits anchorage-independent growth in Ewing sarcoma cells. A.** Soft agar assays in A673 cells following knockdown of EWS-FLI1, EWSR1, or scramble control. **B.** Bar graph quantifies relative colony count in A673 cells. Error bars represent standard deviation. (n = 3). **C.** Soft agar assays in HEK293T/17 cells with control and knockdown treatments. **D.** Bar graph quantifies relative colony count in HEK293T/17 cells. Error bars represent standard deviation about the mean (n = 4). Student's t-test was calculated assuming equal variances: ** $p < 0.01$; * $p < 0.05$; n.s., no significance ($p > 0.05$).

We next asked whether EWSR1 was required for growth on soft agar in a cell line lacking the EWS-FLI1 fusion protein. We chose HEK293T/17 cells, which also does not express detectable levels of FLI1 protein. Transfection with siEWSR1 effectively diminished EWSR1 protein but siEF had no effect (**Supplemental Figure S2E**). HEK293T/17 cells treated with siEWSR1, siEF, or the siSCR control produced similar colony numbers on soft agar (n = 4, $p > 0.05$, Student's t-test, **Figure 2C** and **2D**). This result raised the possibility that the role of EWSR1 may be modified by EWS-FLI1 in the cell.

Noting that the EWSR1 knockdown did not produce an effect on HEK293T/17 growth on the soft agar, we asked if introducing the fusion protein would reproduce the result observed in Ewing sarcoma

cells. We expressed V5-tagged EWS-FLI1 protein in HEK293T/17 cells (**Supplemental Figure S3A**). HEK293T/17 cells expressing the fusion protein produced 60% fewer colonies after the loss of EWSR1 and compared to the siSCR-treated control (n = 6, $p < 0.001$, Student's t-test, **Figure 3A** and **3B**). We considered whether EWS-FLI1 effects on EWSR1 involved the direct interaction between the proteins in HEK293T/17 cells[9,26,34]. Using immunoprecipitation (IP) with antibodies that bind EWSR1 and not the fusion protein, western blot assays indicated EWS-FLI1 protein eluted with EWSR1 but not the non-specific IgG control IP (**Supplemental Figure S3B**). These experiments confirmed the presence of the physical interaction between EWS-FLI1 and EWSR1 in the HEK293T/17 cells that were changed to become sensitive to the loss of EWSR1.

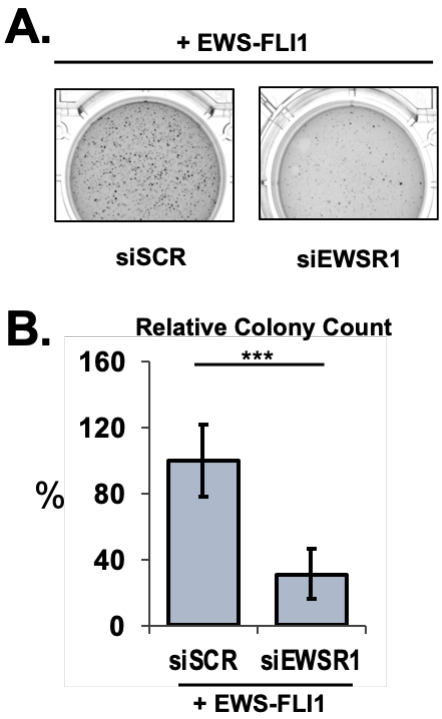


**Figure 3. Expression of EWS-FLI1 in HEK293T/17 cells recapitulates loss of EWSR1 phenotype. A.** Soft agar assays of HEK293T/17 cells co-transfected with V5-EWS-FLI1 and siEWSR1 or V5-EWS-FLI1 and control siRNA, siSCR (n = 6). **B.** Quantification of relative colony number from soft agar assays. Error bars represent standard deviation about the mean. Student's *t*-test was calculated for assuming equal variances: *** $p < 0.001$.

**EWSR1 and RNA Pol II associate with protein granules in cells**

The low-complexity domain shared by FET proteins and fusion proteins driving Ewing sarcoma are capable of undergoing phase separation, which is tied to the formation of granule bodies in cells[28,41,42]. All three FET proteins bind RNA Pol II to regulate transcription[5,8,43]. We previously reported a granular body comprised of FUS and RNA Pol II[37]. Consistent with the weak interactions found for products of phase separation *in vitro*, granules could not survive lysis unless stabilized by formaldehyde crosslinking[44,45]. Now we tested if EWSR1 was also found in a granule in cells.

We used a separation-based approach and HEK293T/17 cells to characterize the size of protein particles containing EWSR1 and RNA Pol II, with or without formaldehyde crosslinking[46]. Nucleic acids were depleted by sonication and nuclease treatment before lysates were passed through size-exclusion chromatography (SEC) using a CL-2B column, which can separate particles up to 250 nm in diameter. UV absorption indicated most cellular proteins to be present in fractions eluting after 20 mL, which was expected for monomers and complexes less than 20 nm in diameter (n = 3, **Supplemental Figure S4A**). UV absorption indicated that formaldehyde crosslinking did not appreciably change the elution of most cellular proteins, indicating most proteins were not in large particles or granules that could be stabilized by formaldehyde crosslinking (n = 3, **Figure 4A**, top).

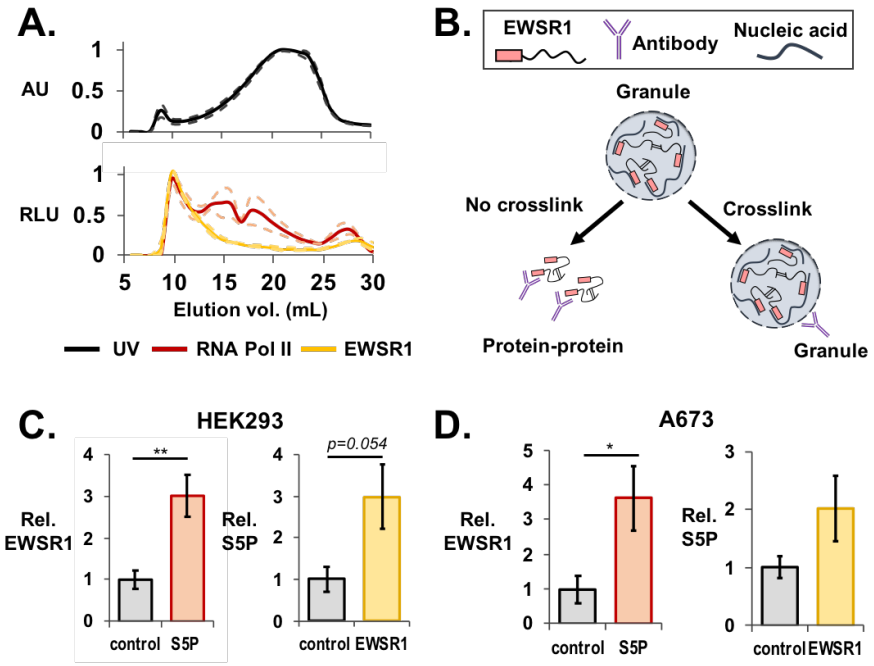


**Figure 4. EWSR1 and RNA Pol II assemble into large protein granules. A.** (Top) UV absorbance trace of crosslinked HEK293T/17 cell lysates. (Bottom) Elution profile of RNA Pol II and EWSR1 from crosslinked HEK293T/17 cells as determined by ELISA during SEC by CL-2B column. Dashed lines represent standard error. (n = 3). **B.** Diagram of crosslinked IP versus non-crosslinked IP. **C.** Crosslinked immunoprecipitation assay of phosphorylated Ser5 in the CTD heptad repeat of RNA Pol II (S5P) and EWSR1 in HEK293T cells. (n = 3). **D.** Crosslinked immunoprecipitation assay phosphorylated Ser5 in the CTD heptad repeat of RNA Pol II (S5P) and EWSR1 in A673 cells. immunoprecipitates with RNA Pol II in crosslinked granules. Error bars represent standard error about the mean (n = 3). AU = absorbance units. RLU = relative luminescence units. Student's *t*-test was calculated for assuming equal variances: ** $p < 0.01$; * $p < 0.05$; n.s., no significance ($p > 0.05$). For **C-D**, Protein G beads served as the negative control.

SEC fractions were probed for RNA Pol II and EWSR1 by ELISA assays, since formaldehyde crosslinking interferes with the SDS-PAGE step for western assays. The largest diameter of the RNA Pol II holoenzyme is 25 nm and we found its elution in un-crosslinked cells to be maximal near the expected

volume of 18 to 20 mL (**Supplemental Figure S4B**). EWSR1 eluted at >20 mL, indicating smaller protein particles or monomers. Formaldehyde crosslinking resulted in RNA Pol II eluting at volumes <15 mL, which indicates particles of 50 to >150 nm in diameter (**Figure 4A**). Most EWSR1 protein was detected to elute in large particles.

We tested whether EWSR1 and RNA Pol II were crosslinked together HEK293T/17 cells. RNA Pol II was immunoprecipitated using an antibody specific for its Serine-5 phosphorylated form (S5P). Significant enrichment for EWSR1 eluting with the polymerase was observed in ELISA assays, relative to a protein G bead negative IP control ($n = 3$, $p = 0.009$, Student's *t*-test, **Figure 4C**, left). By IP for EWSR1, we also found enrichment for S5P RNA Pol II ($n = 3$, $p = 0.05$, Student's t-test, **Figure 4C**, right). We repeated the IP assay for crosslinked A673 lysates, which confirmed the interaction of EWSR1 and RNA Pol II in Ewing sarcoma cells ($n = 3$, $p = 0.04$, Student's t-test, **Figure 4D**).

**EWS-FLI1 is found in a protein granule in cells**

We have previously used transmission electron microscopy to image crosslinked protein particles immunopurified from cell lysates[37]. We asked if this approach could confirm whether EWS-FLI1 was present in a large protein body in cells. First, we tested whether crosslinked EWS-FLI1 retained its interactions with EWSR1 and RNA Pol II.

We performed IP assays from HEK293T/17 cells transfected with V5-tagged EWS-FLI1. By ELISA assay, EWS-FLI1 was found highly enriched in eluates from EWSR1 IP experiments over negative protein G bead controls ($n = 3$, $p = 0.01$, Student's t-test, **Figure 5A**). EWS-FLI1 was likewise enriched in RNA Pol II IP experiments over negative controls ($n = 3$, $p = 0.03$, Student's t-test, **Figure 5A**). We tested whether the ability for EWS-FLI1 to oligomerize might potentially play a role in its ability to bind EWSR1 or RNA Pol II. Replacing the tyrosine residues with serine in the repeated [S/G]Y[S/G] motif of the LC-domain can prevent oligomerization[8,28]. We transfected in HEK293T/17 cells a V5-tagged EWS-FLI1 construct with 37 tyrosine residues replaced by serine (YS37). Expression for YS37 was comparable to that of wild-type EWS-FLI1 (**Supplemental Figure S5A and S5B**). However, IP assays for EWSR1 or RNA Pol II failed

to recover the YS37 fusion protein (n = 3, p > 0.05, Student's t-test, **Figure 5B**). This result suggested that the oligomerization found during phase separation may be required for the fusion protein to interact with EWSR1 or RNA Pol II in cells. We also tested whether EWSR1 and RNA Pol II crosslinked and pulled down with the endogenous EWS-FLI1 protein in A673 cells, which is expressed at lower levels comparted to western blots from HEK293T/17 **(Supplemental Figure 3A).** In the Ewing sarcoma cell line, EWS-FLI1 also eluted with EWSR1 or RNA Pol II at levels enriched over negative controls (n = 4, p < 0.05, Student's t-test, **Figure 5C**). In the reciprocal EWS-FLI1 IP in HEK293T/17 and A673 cells, we observed enrichment of EWSR1 and RNA Pol II but did not find enrichment in the IP of the YS37 variant of EWS-FLI1 (**Supplemental Figure S5C-S5F**).

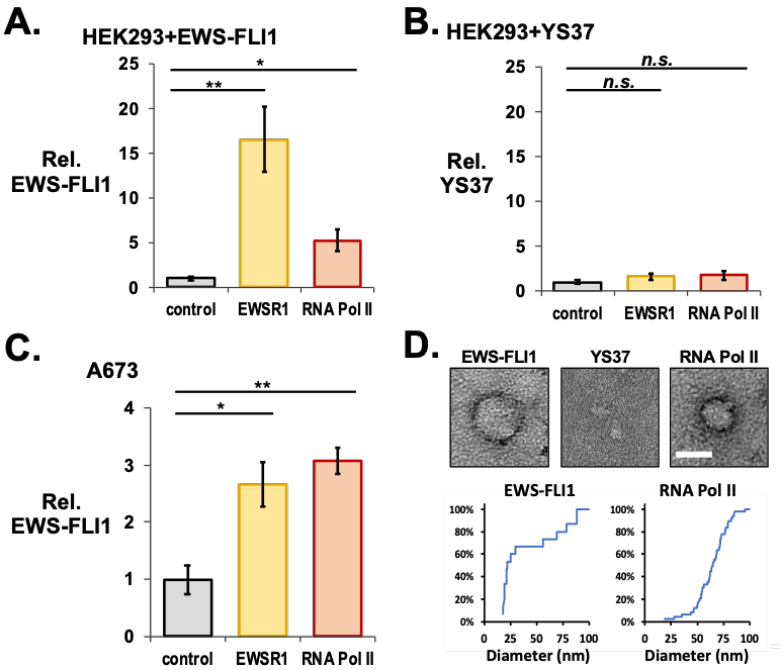


**Figure 5. EWS-FLI1 and RNA Pol II coimmunoprecipitate in crosslinked protein granules.**

**A.** Crosslinked immunoprecipitation assay of RNA Pol II and EWSR1 from HEK293T/17 cells transfected with EWS-FLI1. EWS-FLI1 immunoprecipitated with endogenous EWSR1 and RNA Pol II. Error bars represent standard error. (n = 3) **B.** Crosslinked immunoprecipitation assay of HEK293T/17 cells transfected with the YS37 mutant of EWS-FLI1. Error bars represent standard error. (n = 3) **C.** Crosslinked

immunoprecipitation assay of A673 cells. Endogenous EWS-FLI1 immunoprecipitated with EWSR1 and RNA Pol II. Error bars represent standard error (n = 4). **D.** Transmission electron microscopy of immunoprecipitated EWS-FLI1, YS37, and RNA Pol II particles (Scale bar = 50 nm). Diameters of particles for EWS-FLI1 (n = 24) or RNA Pol II (n = 77) are shown as cumulative plots. Student's *t*-test was calculated for assuming equal variances: ** $p < 0.01$; * $p < 0.05$; n.s., no significance ($p > 0.05$). For **A-C**, Protein G beads served as the negative control.

Finally, we investigated whether the IP assays from crosslinked HEK293T/17 lysates recovered granular bodies. We used negative-stained transmission electron microscopy (TEM) to image particles recovered by IP of RNA Pol II in HEK293T/17 cells, which we had previously reported[37]. We observed round particles up to 95 nm in diameter recovered in the RNA Pol II IP samples. RNA Pol II holoenzyme would be expected to appear as particle of 15-25 nm in size. Particles of the size of the polymerase or larger were observed to have an average diameter of 64 ± 15 nm (n = 77, **Figure 5D**). We confirmed that particles observed were comprised of protein by treating samples with proteinase K, which eliminated the round particles observed during TEM (**Supplemental Figure S6**).

We tested whether particles were also observable in EWS-FLI1 IP samples from crosslinked lysates of HEK293T/17 cells that expressed V5-EWS-FLI1. Round particles were observed by TEM to elute from the IP of EWS-FLI1 (**Figure 5D,** middle panels). The EWS-FLI1 associated particles were found across a broader range of sizes with an averaged diameter of 42 ± 27 nm in diameter (n = 24). To test whether the particles were specific for EWS-FLI1 and the fusion protein's ability to oligomerize by homotypic interactions, we performed the same IP experiment and TEM imaging using HEK293T/17 cells expressing the YS37 variant of EWS-FLI1. The IP of the YS37 mutant did not reveal any round particles that were visible to TEM (**Figure 5D**). This was consistent with the expectation for YS37 to be incapable of oligomerization or phase separation.

We have found that EWSR1 and EWS-FLI1 regulate many of the same genes and both are required for Ewing sarcoma cells to maintain growth under anchorage-independent conditions. Expression of the fusion

protein can cause non-Ewing cells to depend on EWSR1 for colony growth in a soft agar assay, which suggests the fusion protein is responsible for the effect EWSR1 had on cell growth. By confirming that EWS-FLI1 and EWSR1 interact in the affected cells, the ability of the fusion protein to modify EWSR1 activity may be the result of protein:protein interactions. To explore the context for interactions formed by EWS-FLI1 or EWSR1, we showed that EWSR1 inhabits large bodies in cells comparable to those for RNA Pol II. Crosslinked EWS-FLI1 was bound to RNA Pol II and EWSR1, but without its tyrosine residues that are required to form oligomers, it could not bind either protein. We used TEM to observe large protein particles that immunopurified with EWS-FLI1 and also appeared similar to those associated with RNA Pol II. Again, the tyrosine residues in the LC domain was required to observe the crosslinked particles after immunopurification. This reveals a new property of EWS-FLI1, the ability of its LC domain to self-assemble allows it to associate with protein particles similar in size and appearance as those found for EWSR1 and RNA Pol II. Taken together, interactions between these proteins may occur in the context of a nuclear granule formed by the protein assemblies.

## DISCUSSION

EWSR1 and EWS-FLI1 each contain the same disordered domain with a capacity for self-oligomerization. Results of this study support a model that EWS-FLI1 and EWSR1 regulate transcription for hundreds of identical gene targets. EWSR1 and the fusion protein are each required to maintain the signature property of transformation, anchorage-independent proliferation. In addition to these shared functional capacities, these proteins interact physically with each other. EWSR1 is found almost entirely in large particles in the cell, like those containing RNA Pol II. We also find that EWS-FLI1 and RNA Pol II associate with particles of similar size and appearance when analyzed with TEM. This is consistent with the hypothesis that the ability of EWS-FLI1 to self-oligomerize may tie its function in cells to protein granules. The conclusion of this study offers new support to the model that interactions made by EWS-FLI1 occur in the context of a higher-order structure rather than traditional macromolecular complexes[8,9,26,34,38].

We found EWS-FLI1 affected transcript levels for nearly half the genes whose transcripts were also affected by EWSR1. EWS-FLI1 has an ability to either increase or reduce transcript levels for affected genes (**Figure 1B**). Several mechanisms may contribute to the ability of EWS-FLI1 to alternate its effects on transcription. EWS-FLI1 has been noted to bind both activator and repressor complexes and its interacting partners may depend on the sites in genomic DNA where the fusion protein binds[24–26]. The effects of EWSR1 on genes also targeted by the fusion protein are remarkably similar. Our result that hundreds of genes can be affected by both EWS-FLI1 and EWSR1 may be a lower estimate, since EWSR1 concentrations in the cell are quite high (~8 μM) and proteomics studies have indicated levels of endogenous EWS-FLI1 to be much lower[47–49]. Consequently, siRNA knockdown may more effectively abolish the activity of EWS-FLI1, resulting in effects that were seen for more genes and changes to transcript levels that were generally greater than those found with the EWSR1 knockdown.

In addition to a large number of genes that were affected by both EWSR1 and EWS-FLI1, the capacity for anchorage-independent growth was affected by both proteins, which extends the functions in common for the fusion and wild-type proteins to include cellular functions (**Figure 2A**). A role for EWSR1 in this aspect of cell growth is not typical of transformed cells, as we have shown for HEK293T/17 cells (**Figure 2C**). However, expression of EWS-FLI1 from a transfected plasmid was sufficient to reproduce the dependence of cell proliferation on EWSR1 (**Figure 3**). This result is consistent with a hypothesis that EWS-FLI1 can modify EWSR1 function in the cell. We confirmed the interaction between the proteins in transfected HEK293T/17 cells, which offers at least one basis to explain the functional relationship between the proteins (**Supplemental Figure S3B**).

Having seen the potential importance of interactions between EWSR1 and EWS-FLI1, we investigated the characteristics of protein interactions made by EWSR1, RNA Pol II, and EWS-FLI1 in cells. An ordinary protein interaction would be expected to result in a discrete macromolecular complex. Examples of these might range from the dimeric interactions typical of steroid hormone receptors to the 48-mer structure of the 26S proteasome or the RNA Pol II holoenzyme itself. However, EWSR1 and EWS-FLI1

have been shown to oligomerize into higher-order assemblies[8,34]. Examples of such assembles can include those with distinctive structures, such as actin fibers and nuclear pore complexes[50,51]. Higher-order assemblies also include those that result from a form of phase separation whose weak multivalent interactions produce rounded amorphous shapes reminiscent of a liquid drop in suspension[42,52,53]. As seen for studies with recombinant LC domain proteins, the EWS-FLI1 particles we recovered from cells have the appearance of the liquid-like phase separation of a protein or ribonucleoprotein granule (**Figure 5D**).

FET proteins contain a low complexity domain that is intimately tied to normal cell processes and disease states. Ewing sarcoma is an example where wild-type and aberrant LC domain proteins exist and interact in the same system. The multivalent interactions driving LC domain assembly form through π-bonds involving tyrosine residues in the repeated [S/G]Y[S/G] motifs[44,45,54–56]. Tyrosine-rich LC domains are found in many RNA-binding proteins of the hnRNP family, which can allow these proteins to undergo phase separation together through homotypic interactions. We could confirm that the interactions of EWS-FLI1 with EWSR1 or RNA Pol II required these tyrosine residues (**Figure 5B**). The same was true for the assembly of EWS-FLI1 into protein granules that were seen with TEM (**Figure 5D**). This suggests that the protein is functional when it can form higher-order assemblies. Because EWS-FLI1 binding partners are found in similar protein bodies in the cell, their interactions with each other may be through assembly into a granule together.

The inclusion of fusion proteins driving Ewing sarcoma into granules like those observed for FET proteins and RNA Pol II raises exciting new questions to be explored. Do all three FET proteins combine in a single protein granule with the fusion protein? Translocations involving a FET protein are an especially common driver mutation in sarcomas, and a FET protein LC domain is found in nearly half of fusion proteins implicated in the disease[14]. The high conservation of three distinct genes throughout vertebrates can argue that they have critical but independent functions. However, the mechanisms that can initiate sarcoma development may lie in an area where the functions of the FET proteins overlap. Secondly, is recruitment of hnRNP proteins and RNA processing machineries common at sites along DNA bound by

FET-fusion proteins, such as EWS-FLI1? If true, this would offer at least three possibilities to explore: localizing RNA processing machinery can enable transcription that promotes tumorigenesis; RNA polymerase can be recruited by RNA processing machinery to initiate transcription of genes; and, transcription may be suppressed for some genes if the fusion protein directs their RNA processing machinery elsewhere. Lastly, since the fusion protein binds and recruits promiscuous RNA-binding proteins, what RNA transcripts interact with the assemblies and what roles might they serve? One key step to explore these questions will be determining the extent that FET-fusion proteins like EWS-FLI1 can inhabit additional nuclear complexes or granules that are not bound to DNA.

**Corresponding Author**

Correspondence should be addressed to Jacob C. Schwartz at jcschwartz@arizona.edu.

**Author Contributions**

N.S.A. designed and performed experiments, analyzed data, and interpreted results. L.M.G. contributed the design and characterization of siRNAs, real-time PCR, and protocols involving recombinant DNA. N.S.A. wrote the first draft of the manuscript and N.S.A. and J.C.S. collaborated to write subsequent drafts. All authors have approved to the final version of the manuscript.

**Funding Sources and Acknowledgements**

This work was supported by funding from the National Institutes of Health (R21CA238499) and the American Cancer Society (RSG-18-237-01-DMC) to J.C.S. Next-generation sequencing was performed by the University of Arizona Genetics Core, http://uagc.arizona.edu. Transmission election microscopy was performed with the Eyring Materials Center at Arizona State University, supported in part by NNCI-ECCS-1542160. Transmission Electron Microscopy was also performed through the University of Arizona Office of Research, Innovation, & Impact Imaging Cores. Research reported in this publication was also supported by the Office of the Director, National Institutes of Health of the National Institutes of Health, under award number S10OD013237.

**REFERENCES**


1. Schwartz, J. C., Cech, T. R. & Parker, R. R. Biochemical Properties and Biological Functions of FET Proteins. *Annu. Rev. Biochem.* **84**, 355–379 (2015).
2. Ozdilek, B. A. *et al*. Intrinsically disordered RGG/RG domains mediate degenerate specificity in RNA binding. *Nucleic Acids Res.* **45**, (2017).
3. Luo, Y. *et al*. EWS and FUS bind a subset of transcribed genes encoding proteins enriched in RNA regulatory functions. *BMC Genomics* **16**, 1–17 (2015).
4. Masuda, A. *et al*. Position-specific binding of FUS to nascent RNA regulates mRNA length. *Genes Dev.* **29**, 1045–1057 (2015).
5. Schwartz, J. C. *et al*. FUS binds the CTD of RNA polymerase II and regulates its phosphorylation at Ser2. *Genes Dev.* **26**, 2690–2695 (2012).
6. Hoell, J. I. *et al*. RNA targets of wild-type and mutant FET family proteins. *Nat. Struct. Mol. Biol.* **18**, 1428–1431 (2011).
7. Schwartz, J. C., Wang, X., Podell, E. R. & Cech, T. R. RNA Seeds Higher-Order Assembly of FUS Protein. *Cell Rep.* **5**, (2013).
8. Kwon, I. *et al*. XPhosphorylation-regulated binding of RNA polymerase II to fibrous polymers of low-complexity domains. *Cell* **155**, 1049 (2013).
9. Gorthi, A. *et al*. EWS-FLI1 increases transcription to cause R-loops and block BRCA1 repair in Ewing sarcoma. *Nature* **555**, 387–391 (2018).
10. Chi, B. *et al*. Interactome analyses revealed that the U1 snRNP machinery overlaps extensively with the RNAP II machinery and contains multiple ALS/SMA-causative proteins. *Sci Rep* **8**, 8755 (2018).
11. Yang, L., Chansky, H. A. & Hickstein, D. D. EWSFli-1 Fusion Protein Interacts with Hyperphosphorylated RNA Polymerase II and Interferes with Serine-Arginine Protein-mediated RNA Splicing*. (2000). doi:10.1074/jbc.M005739200
12. Paronetto, M. P., Miñana, B. & Valcárcel, J. The Ewing Sarcoma Protein Regulates DNA

Damage-Induced Alternative Splicing. *Mol. Cell* **43**, 353–368 (2011).

13. Rogelj, B. *et al*. Widespread binding of FUS along nascent RNA regulates alternative splicing in the brain. *Sci. Rep*. **2**, 1–10 (2012).

14. Riggi, N., Cironi, L., Suvà, M.-L. & Stamenkovic, I. Sarcomas: genetics, signalling, and cellular origins. Part 1: The fellowship of TET. *J. Pathol*. **213**, 4–20 (2007).

15. Tan, A. Y. & Manley, J. L. The TET family of proteins: functions and roles in disease. *J Mol Cell Biol* **1**, 82–92 (2009).

16. Delattre, O. *et al*. Gene fusion with an ETS DNA-binding domain caused by chromosome translocation in human tumours. *Nature* **359**, 162–165 (1992).

17. Grünewald, T. G. P. *et al*. Ewing sarcoma. *Nature Reviews Disease Primers* **4**, (2018).

18. Riggi, N. *et al*. Development of Ewing's sarcoma from primary bone marrow-derived mesenchymal progenitor cells. *Cancer Res*. **65**, 11459–11468 (2005).

19. Riggi, N. *et al*. EWS-FLI-1 expression triggers a ewing's sarcoma initiation program in primary human mesenchymal stem cells. *Cancer Res*. **68**, 2176–2185 (2008).

20. Kovar, H. *et al*. EWS/FLI-1 antagonists induce growth inhibition of Ewing tumor cells in vitro. *Cell Growth Differ*. **7**, 429–437 (1996).

21. Tanaka, K., Iwakuma, T., Harimaya, K., Sato, H. & Iwamoto, Y. EWS-Fli1 antisense oligodeoxynucleotide inhibits proliferation of human Ewing's sarcoma and primitive neuroectodermal tumor cells. *J. Clin. Invest*. **99**, 239–247 (1997).

22. Gangwal, K. *et al*. Microsatellites as EWS/FLI response elements in Ewing's sarcoma. *Proc. Natl. Acad. Sci. U. S. A*. **105**, 10149–10154 (2008).

23. Bailly, R. A. *et al*. DNA-binding and transcriptional activation properties of the EWS-FLI-1 fusion protein resulting from the t(11;22) translocation in Ewing sarcoma. *Mol. Cell. Biol*. **14**, 3230–3241 (1994).

24. Sankar, S. *et al*. Mechanism and relevance of EWS/FLI-mediated transcriptional repression in Ewing sarcoma. *Oncogene* **32**, 5089–5100 (2013).

25. Riggi, N. *et al*. EWS-FLI1Utilizes Divergent Chromatin Remodeling Mechanisms to Directly Activate or Repress Enhancer Elements in Ewing Sarcoma. *Cancer Cell* **26**, 668–681 (2014).

26. Boulay, G. *et al*. Cancer-Specific Retargeting of BAF Complexes by a Prion-like Domain. *Cell* **171**, 163-178.e19 (2017).

27. Selvanathan, S. P. *et al*. EWS–FLI1 modulated alternative splicing of ARID1A reveals novel oncogenic function through the BAF complex. *Nucleic Acids Res*. **47**, 9619–9636 (2019).

28. Kato, M. *et al*. Cell-free formation of RNA granules: Low complexity sequence domains form dynamic fibers within hydrogels. *Cell* **149**, 753–767 (2012).

29. Schwartz, J. C., Wang, X., Podell, E. R. & Cech, T. R. RNA Seeds Higher-Order Assembly of FUS Protein. *Cell Rep*. **5**, 918–925 (2013).

30. Boeynaems, S. *et al*. Protein Phase Separation: A New Phase in Cell Biology. *Trends in Cell Biology* **28**, 420–435 (2018).

31. Jain, S. *et al*. ATPase-Modulated Stress Granules Contain a Diverse Proteome and Substructure. *Cell* **164**, 487–498 (2016).

32. West, J. A. *et al*. Structural, super-resolution microscopy analysis of paraspeckle nuclear body organization. *J. Cell Biol*. **214**, 817–830 (2016).

33. Blechingberg, J., Luo, Y., Bolund, L., Damgaard, C. K. & Nielsen, A. L. Gene Expression Responses to FUS, EWS, and TAF15 Reduction and Stress Granule Sequestration Analyses Identifies FET-Protein Non-Redundant Functions. *PLoS One* **7**, (2012).

34. Chong, S. *et al*. Imaging dynamic and selective low-complexity domain interactions that control gene transcription. *Science (80-. )*. **361**, (2018).

35. Spahn, L. *et al*. Homotypic and heterotypic interactions of EWS, FLI1 and their oncogenic fusion protein. *Oncogene* **22**, 6819–6829 (2003).

36. Embree, L. J., Azuma, M. & Hickstein, D. D. Ewing sarcoma fusion protein EWSR1/FLI1 interacts with EWSR1 leading to mitotic defects in zebrafish embryos and human cell lines. *Cancer Res*. **69**, 4363–4371 (2009).

37. Thompson, V. F. *et al*. Transcription-Dependent Formation of Nuclear Granules Containing FUS and RNA Pol II. (2018). doi:10.1021/acs.biochem.8b01097

38. Johnson, K. M. *et al*. Role for the EWS domain of EWS/FLI in binding GGAA-microsatellites required for Ewing sarcoma anchorage independent growth. *Proc. Natl. Acad. Sci.* **114**, 9870–9875 (2017).

39. Smith, R. *et al*. Expression profiling of EWS/FLI identifies NKX2.2 as a critical target gene in Ewing's sarcoma. *Cancer Cell* **9**, 405–416 (2006).

40. Chaturvedi, A., Hoffman, L. M., Welm, A. L., Lessnick, S. L. & Beckerle, M. C. The EWS/FLI Oncogene Drives Changes in Cellular Morphology, Adhesion, and Migration in Ewing Sarcoma. *Genes and Cancer* **3**, 102–116 (2012).

41. Kato, M. & McKnight, S. L. A Solid-State Conceptualization of Information Transfer from Gene to Message to Protein. *Annu Rev Biochem* (2017). doi:10.1146/annurev-biochem-061516-044700

42. Lin, Y., Protter, D. S., Rosen, M. K. & Parker, R. Formation and Maturation of Phase-Separated Liquid Droplets by RNA-Binding Proteins. *Mol Cell* **60**, 208–219 (2015).

43. Yang, L., Chansky, H. A. & Hickstein, D. D. EWS·Fli-1 fusion protein interacts with hyperphosphorylated RNA polymerase II and interferes with serine-arginine protein-mediated RNA splicing. *J. Biol. Chem.* **275**, 37612–37618 (2000).

44. Wang, J. *et al*. A Molecular Grammar Governing the Driving Forces for Phase Separation of Prion-like RNA Binding Proteins. *Cell* **174**, 688-699 e16 (2018).

45. Qamar, S. *et al*. FUS Phase Separation Is Modulated by a Molecular Chaperone and Methylation of Arginine Cation-pi Interactions. *Cell* **173**, 720-734 e15 (2018).

46. Thompson, V. F. *et al*. Transcription-Dependent Formation of Nuclear Granules Containing FUS and RNA Pol II. *Biochemistry* **57**, 7021–7032 (2018).

47. Gierisch, M. E. *et al*. USP19 deubiquitinates EWS-FLI1 to regulate Ewing sarcoma growth. *Sci. Rep.* **9**, (2019).

48. Elzi, D. J., Song, M., Hakala, K., Weintraub, S. T. & Shiio, Y. Proteomic analysis of the EWS-Fli-

1 interactome reveals the role of the lysosome in EWS-Fli-1 turnover. *J. Proteome Res*. (2014). doi:10.1021/pr500387m

49. Hein, M. Y. *et al*. A Human Interactome in Three Quantitative Dimensions Organized by Stoichiometries and Abundances. *Cell* (2015). doi:10.1016/j.cell.2015.09.053

50. Hughes, M. P. *et al*. Atomic structures of low-complexity protein segments reveal kinked b sheets that assemble networks. *Science (80-. )*. (2018). doi:10.1126/science.aan6398

51. Wu, H. & Fuxreiter, M. The Structure and Dynamics of Higher-Order Assemblies: Amyloids, Signalosomes, and Granules. *Cell* (2016). doi:10.1016/j.cell.2016.05.004

52. Banani, S. F. *et al*. Compositional Control of Phase-Separated Cellular Bodies. *Cell* (2016). doi:10.1016/j.cell.2016.06.010

53. Molliex, A. *et al*. Phase separation by low complexity domains promotes stress granule assembly and drives pathological fibrillization. *Cell* **163**, 123–133 (2015).

54. Hughes, M. P. *et al*. Atomic structures of low-complexity protein segments reveal kinked beta sheets that assemble networks. *Science (80-. )*. **359**, 698–701 (2018).

55. Murray, D. T. *et al*. Structure of FUS Protein Fibrils and Its Relevance to Self-Assembly and Phase Separation of Low-Complexity Domains. *Cell* (2017). doi:10.1016/j.cell.2017.08.048

56. Lin, Y., Currie, S. L. & Rosen, M. K. Intrinsically disordered sequences enable modulation of protein phase separation through distributed tyrosine motifs. *J Biol Chem* **292**, 19110–19120 (2017).